

# Developmental characteristics of cutaneous telocytes in late embryos of the silky fowl

Hao Li,<sup>1,2</sup> Junliang Chen,<sup>1</sup> Wenjun You,<sup>1</sup> Yizhen Xu,<sup>1</sup> Yaqiong Ye,<sup>1</sup> Haiquan Zhao,<sup>1</sup> Junxing Li,<sup>2</sup> Hui Zhang<sup>1,3</sup>

<sup>1</sup>College of Life Science and Engineering, Foshan University, Foshan

<sup>2</sup>Institute of Animal Husbandry and Veterinary Science, Zhejiang Academy of Agricultural Sciences, Hangzhou

<sup>3</sup>College of Animal Science and Technology, Jiangxi Agricultural University, Nanchang, China

## ABSTRACT

Telocytes (TCs) have been identified in various animals. However, information on TCs in the embryos is still very limited. In this work, the developing skin of the silky fowl was sampled for TCs identification by histology, immunohistochemistry and transmission electron microscopy. In addition, morphological parameters of cutaneous TCs and their location relationships were measured using a morphometry software – ImageJ (FiJi). At the 12<sup>th</sup>, 16<sup>th</sup> and 20<sup>th</sup> day of incubation, in the embryonic skin, telocyte-like cells (TC-L) were observed in the dermis. TCs were PDGFR $\alpha$ <sup>+</sup> at the 12<sup>th</sup>, 16<sup>th</sup> and 20<sup>th</sup> day of incubation, but showed CD34<sup>+</sup> only at 20<sup>th</sup> day of incubation in the embryonic dermis. Ultrastructurally, TCs were observed in the dermis at all late embryonic developmental stages. TCs established the homocellular contacts/plasmalemmal adhesion with each other. TCs established heterocellular contacts with melanocytes at 20<sup>th</sup> day of incubation in the dermis. In addition, the intracellular microvesicles were present in the cytoplasm of TCs. The extracellular microvesicles/exosomes were in close proximity to the TCs. The results confirmed that the locations, immunophenotypes, structural characteristics and relationships of TCs, and revealed the developmental characteristics of cutaneous TCs in late silky fowl embryos.

**Key words:** chicken; embryo; skin; telocyte; development.

**Correspondence:** Hui Zhang, College of Life Science and Engineering, Foshan University, Foshan 528231, China. E-mail: zhanghui429@hotmail.com

**Contributions:** HZhang, conceptualization, supervision, funding acquisition; YY, HZ, JL, HZhang, methodology; HL, JC, HZhang, software; JC, HL, WY, YX, investigation; HL, HZhang, manuscript drafting; HZHANG, JL, manuscript review and editing.

**Conflict of interest:** the authors declare that they have no competing interests.

**Ethics approval:** this study was approved by the Animal Ethical Committee of Foshan University (Foshan, China; approval no. Fosu2022038).

**Availability of data and materials:** the data supporting the findings of this study are available from the corresponding author upon reasonable request.

**Funding:** this work was supported by the National Natural Science Foundation of China (31760716; 31560681), the Project of Jiangxi Province (20151BBF60007; 20171ACB21028) and the Cooperative Project from Foshan University and Zhejiang Academy of Agricultural Sciences (BKH209071; BKH20907101).

## Introduction

Telocytes (TCs) are a type of interstitial cells characterized by the presence of a specific type of prolongations, termed telopodes (Tps), which are long, slender, uneven and appear as moniliform aspect.<sup>1</sup> Through their intercellular contacts/junctions and extracellular vesicles/exosomes, TCs are proposed to be involved in many physiological functions,<sup>2-5</sup> such as mechanical support, intercellular communication, maintenance and modulation of tissue homeostasis, neurotransmission, immunomodulation and immunosurveillance, and control, regulation and source of other cell types.<sup>6,7</sup> In particular, TCs are an emerging component of the stem cell niche and serve as a nurse to regulate stem cells.<sup>8</sup> Currently, some studies have demonstrated that Lgr5 villus tip TCs act as regulators of the epithelial spatial expression programs along the villus axis.<sup>9</sup> Furthermore, TCs are necessary for maintenance of villus tip endothelial cell polarization and fenestration.<sup>10</sup> Therefore, TCs are considered to play a role in angiogenesis and tissue regeneration/repair, and they could exert their influence in cellular therapy and organ regeneration.<sup>1,8,9,11,12</sup>

In pathology, TCs play complex roles in various diseases, including tumour,<sup>13-15</sup> endometriosis,<sup>16</sup> ectopic pregnancy,<sup>17</sup> and fibrosis diseases.<sup>18</sup> In addition, TCs are involved in skin pathology.<sup>19</sup> For example, the sensitivity of infantile haemangiomas to propranolol may be due to cross-talk between lesional vascular cells and TCs.<sup>20</sup> Furthermore, a previous study indicated that loss of *Pten* in TCs is sufficient to trigger the development of spontaneous colonic polyposis.<sup>21</sup> Dysfunction of TCs reprograms the gut's microenvironment and drives the intestinal epithelium towards colonic pathologies.<sup>22</sup> These findings further support that signalling silenced TCs have an altered stromal cell ratio and secretory profile, leading to the establishment of a toxic niche that affects epithelial homeostasis. This increasing evidence suggests that TCs are involved in the pathological processes of many diseases.

TCs have been identified in various organs of humans, mammals, birds and poikilotherms. However, these studies are mainly carried out in adults. Data on TCs in embryos are still very limited. Although TCs have a characteristic ultrastructure in different organs of humans and animals, they present immunophenotypic heterogeneity in different anatomical locations.<sup>19,23</sup> Thus, the cellular identity, origin, and nature of TCs remain to be elucidated. The variability of TCs between adult and embryo needs to be further illustrated. Disclosing the spatiotemporal structure characteristics and immunophenotypes is one way to reveal the nature and origin of TCs.

Here, we aimed to record the developmental location pattern and immunophenotypic characteristics of TCs during cutaneous morphogenesis in the late embryos of the silky fowl. In particular, the study illustrates the specific spatio-temporal relationships between TCs and surrounding cell types, such as melanocytes. These results demonstrate that developmental spatio-temporal variation properties of cutaneous TCs of avian late embryos. Furthermore, it contributes to a better understanding of the origin and nature of TCs, and these data may be useful for understanding the physiological roles of TCs in the skin of avian embryos.

## Materials and Methods

### Chicken embryos

Hatching eggs were purchased from a silky fowl farm. Twenty-four chicken eggs were incubated in an incubator at 60-70%

humidity at 37.5-38.5°C. The eggshells were sterilized with 75% ethanol and were knocked broken at the air cell area at the 12<sup>th</sup>, 16<sup>th</sup>, 20<sup>th</sup> day of incubation, respectively. The chicken embryos were removed from the eggs, and then were placed on a Petri dish containing PBS. The embryos were washed with PBS to remove the yolk, and then they were sacrificed by cervical dislocation euthanasia. All animal and embryo procedures were approved by the Animal Ethical Committee of Foshan University (Foshan, China; No. Fosu2022038).

### Collection and treatment of chicken embryo skin tissue materials

After sacrifice, the dorsal skin of embryos was collected. The skin samples were separated and taken, and then they were divided into many small pieces. Some of the skin pieces were fixed in 10% formalin/PBS for 48 h for paraffin section and haematoxylin and eosin (H&E) staining. Some of the skin pieces were fixed in 4% paraformaldehyde/PBS overnight for immunohistochemical method. Other smaller pieces of skin (approximately 1 mm × 2 mm) were fixed in 2.5% glutaraldehyde/PBS overnight for transmission electron microscopy method.

### Histology for telocyte-like cells (TC-L) identification

The skin samples were removed from 10% formalin/PBS, and then they were washed with 0.01 M PBS at pH 7.4. The skin samples were dehydrated in a series of graded concentrations of ethanol. The skin samples were then placed in xylene and embedded in paraffin. The blocks of skin samples were sectioned for histology on a RM2245 microtome (Leica, Wetzlar, Germany). The section thickness was 5 µm. The flattened sections were floated on a slide in a water bath. After dewaxing with xylene, the sections were rehydrated in a gradient of 100% to 70% ethanol, washed with double-distilled H<sub>2</sub>O, and stained with H&E. The sections were dehydrated, mounted and observed using an NLCD500 light microscopy (Nanjing, China).

### CD34 and PDGFR $\alpha$ immunohistochemistry (IHC) for identification of TCs

IHC protocol was performed according to our previous studies.<sup>24</sup> Briefly, the sample sections were deparaffinated in xylene, and were rehydrated in a gradient of 100% to 70% ethanol. The sample sections were washed in PBS. For antigen retrieval, the serial skin sections were put in the sodium citrate buffer (0.1 M, pH=6.0) for 30 min at 95°C. The sample sections were incubated in 3% H<sub>2</sub>O<sub>2</sub>/PBS for 15 min to inactivate endogenous peroxidase at room temperature. All following steps were performed in a moist chamber in a dark environment. The sections were incubated in 5% goat serum/PBS for 20 min at room temperature, and then goat serum was discarded. Immediately, the serial skin sections were incubated overnight with the anti-CD34 (1:50) (MCA5936GA, Bio-Rad Laboratories, Hercules, CA, USA) and PDGFR $\alpha$  (1:200) (LS-C352658, Lsbio, Seattle, WA, USA) antibodies, respectively, at 4°C in a refrigerator. Control skin sections were prepared by the same process except that no primary antibodies were added. The next day, after being washed with PBS, the sections were incubated with biotinylated anti-rabbit IgG (ZSGB-Bio, Beijing, China) at 37°C for 30 min and with streptavidin-horseradish peroxidase working fluid (ZSGB-Bio) at 37°C for 30 min. The color was displayed by 3-amino-9-ethylcarbazole (AEC) (A2010, Solarbio, Beijing, China). The staining was stopped with PBS when positive cells were clearly visible. The sections were then counterstained with haematoxylin and mounted with glycerol jelly mounting medium (Servicebio, China). Finally, the sections were photographed using an NLCD500 light microscopy (Nanjing, China).

## Transmission electron microscopy for ultrastructure of TCs

Transmission electron microscopy (TEM) was performed according to our previous studies.<sup>24</sup> After removal from fixation solution, small pieces of skin tissue (approximately 1 mm × 2 mm) were washed in PBS. The skin samples were postfixed in 1% OsO<sub>4</sub> for 2 h. The skin samples were dehydrated in a gradient of 70% to 100% ethanol, and then were immersed in propylene oxide - araldite mixture for 4 h and finally embedded in araldite. The skin sample blocks were sectioned at 100 nm with a UC7 ultramicrotome (Leica), and the sections were then mounted on cooper-coated grids and were stained with 1% uranyl acetate and Reynold's lead citrate for 20 min. The stained sections were observed with a Tecnai G2 Spirit TEM (FEI, Hillsboro, OR, USA), and the ultrastructural pictures were photographed using a high-resolution digital camera attached to TEM.

## Morphometric analysis

Lengths and thicknesses of Tps, diameters of multivesicular bodies and exosomes were measured using ImageJ (FIJI) software (NIH, Bethesda, MD, USA). The method was carried out according to a previous study.<sup>24</sup> First, a micrograph was opened for distance measurement by the software. The scale was set using the original scale of each micrograph using the "Set Scale" tool from the "Analyze" menu. The scale distance was converted from pixel unit to length unit (μm). The straight distances, diameters of podomers and podoms, and lengths of Tps were scaled by "Straight Line" and "Segmented Line", and then measured in the "Measure" tool of the "Analyze" menu. The data were output and analyzed using Office Excel software (Microsoft, Redmond, WA, USA).

## Results

### TC-L in the skin by H&E staining at different developmental periods of late silky fowl embryos

At the 12<sup>th</sup> day of incubation, in the embryonic skin, the TC-L appeared as elongated spindle shaped with thin processes, and they were located in the dermis (Figure 1A). Some of TC-L were observed close to the epidermis. Others were located near the blood vessels in the deep dermis. The mean length of the processes of TC-L was 8.89 μm (n=4) in the embryonic skin at the 12<sup>th</sup> day of incubation. At the 16<sup>th</sup> day of incubation, in the embryonic skin, thin processes of TC-L were also observed in the dermis of embryonic skin (Figure 1B). The mean length of processes of TC-L was 16.45 μm (n=6). In addition, the mean length of processes of TC-L was 19.50 μm (n=4) in embryonic skin at the 20<sup>th</sup> day of incubation (Figure 1C). Melanocytes were observed close to TCs in the dermis at both 16<sup>th</sup> and 20<sup>th</sup> day of incubation in the embryonic skin (Figure 1 B,C).

### TCs in the skin by IHC at different developmental periods of late silky fowl embryos

In the embryonic skin at the 12<sup>th</sup> day of incubation, TCs did not show a strong CD34 immunopositivity (Figure 2A). However, TCs were located in the dermis and were PDGFR $\alpha$ -immunopositive (Figure 2B). TCs exhibited spindle-shaped with long and thin Tps, which appeared as a moniform aspect with variable thickness (Figure 2B, inset). In the embryonic skin at the 16<sup>th</sup> day of incubation, TCs did not showed strong CD34 immunopositivity (Figure 2D), but showed PDGFR $\alpha$  immunopositivity (Figure 2E) in the dermis. The PDGFR $\alpha$ <sup>+</sup> TCs had thin and long Tps (Figure 2E,

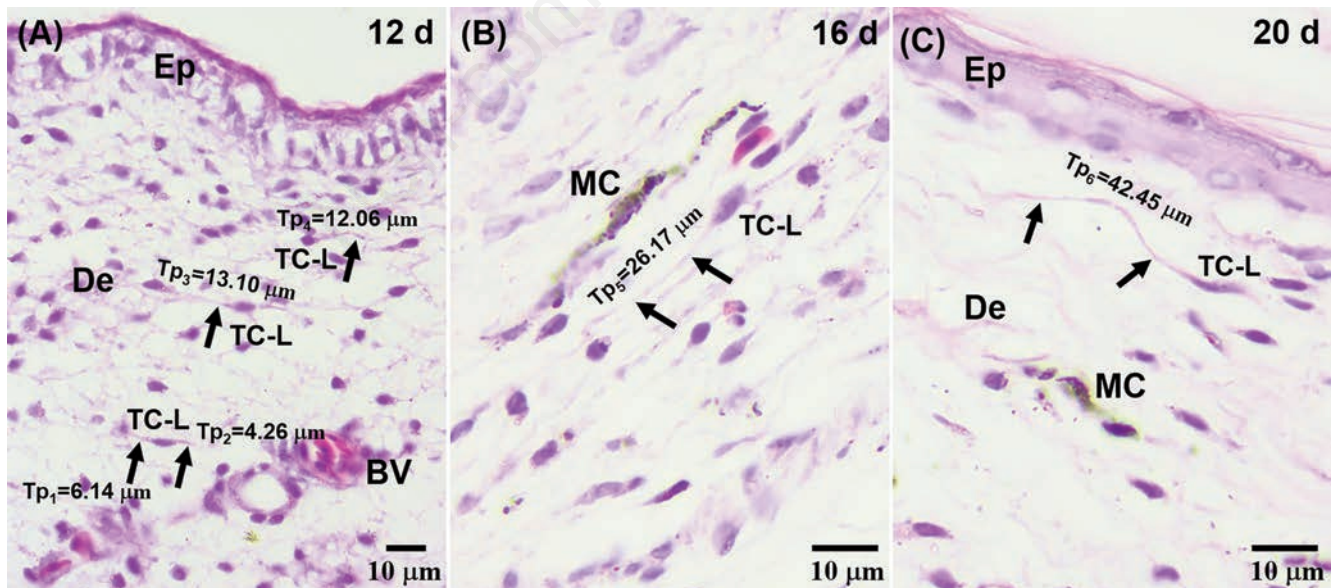


**Figure 1.** Light microscopy microphotographs showing telocyte-like cells (TC-L) by H&E staining in the skin of late embryo of the silky fowl. **A**) TC-L with two thin and long processes (telopode, Tp) (black arrows, lengths = 4.26-13.10 μm) are observed in dermis (De) of the incubation 12-day embryo; Ep, epidermis; BV, blood vessel. **B**) A TC-L with a long Tp (black arrows, length = 26.17 μm) is observed in the dermis of the incubation 16-day embryo; the TC-L is close to a melanocyte (MC). **C**) A TC-L with a long Tp (black arrows, length = 42.45 μm) is observed in the dermis (De) of the incubation 20-day embryo; a melanocyte (MC) is also observed in surrounding area of TC-L; Ep, epidermis.



inset). In the embryonic skin at the 20<sup>th</sup> day of incubation, TCs were both CD34-(Figure 2G) and PDGFR $\alpha$ -immunopositive (Figure 2H) in the dermis. The TCs appeared as spindle-shaped with long and thin Tps (Figure 2 G,H, insets). TCs were also observed in the vicinity of melanocytes (Figure 2 G,H, insets). All negative controls without primary antibodies were not immunopositive (Figure 2 C,F,I).

### Ultrastructural characteristics of TCs in the skin at different developmental periods of late silky fowl embryos

In the embryonic skin at the 12<sup>th</sup> day of incubation, TCs were observed in the dermis (Figures 3 and 4). Some of TCs and their Tps were observed near the base of the epidermis (Figures 4 A,B). TCs

had oval bodies and were mainly occupied by the nuclei (Figures 3 A,B and 4A). The cytoplasm of TCs was sparse and contained small amounts of organelles, such as rough endoplasmic reticulum and mitochondria (Figure 3B). The electron-dense nucleoli were observed close to the side of the nuclei (Figure 3B). TCs had thin and long Tps (Figures 3 and 4). The mean length was 12.65  $\mu$ m (n=4). The thickness of the Tps was approximately 0.11  $\mu$ m. The organelles, rough endoplasmic reticulum and mitochondria, were also observed in the podom of Tps (Figure 4B). TCs/Tps established frequently homocellular close contacts (Figures 3B and 4B). In addition, an extracellular multivesicular body with 1.08  $\mu$ m (n=1) in diameter was observed to adhere closely to the Tps (Figure 3B). Many free shedding vesicles/exosomes with 0.13 $\pm$ 0.04  $\mu$ m (n=6) in diameters were observed in close proximity to the Tps (Figure 3B).

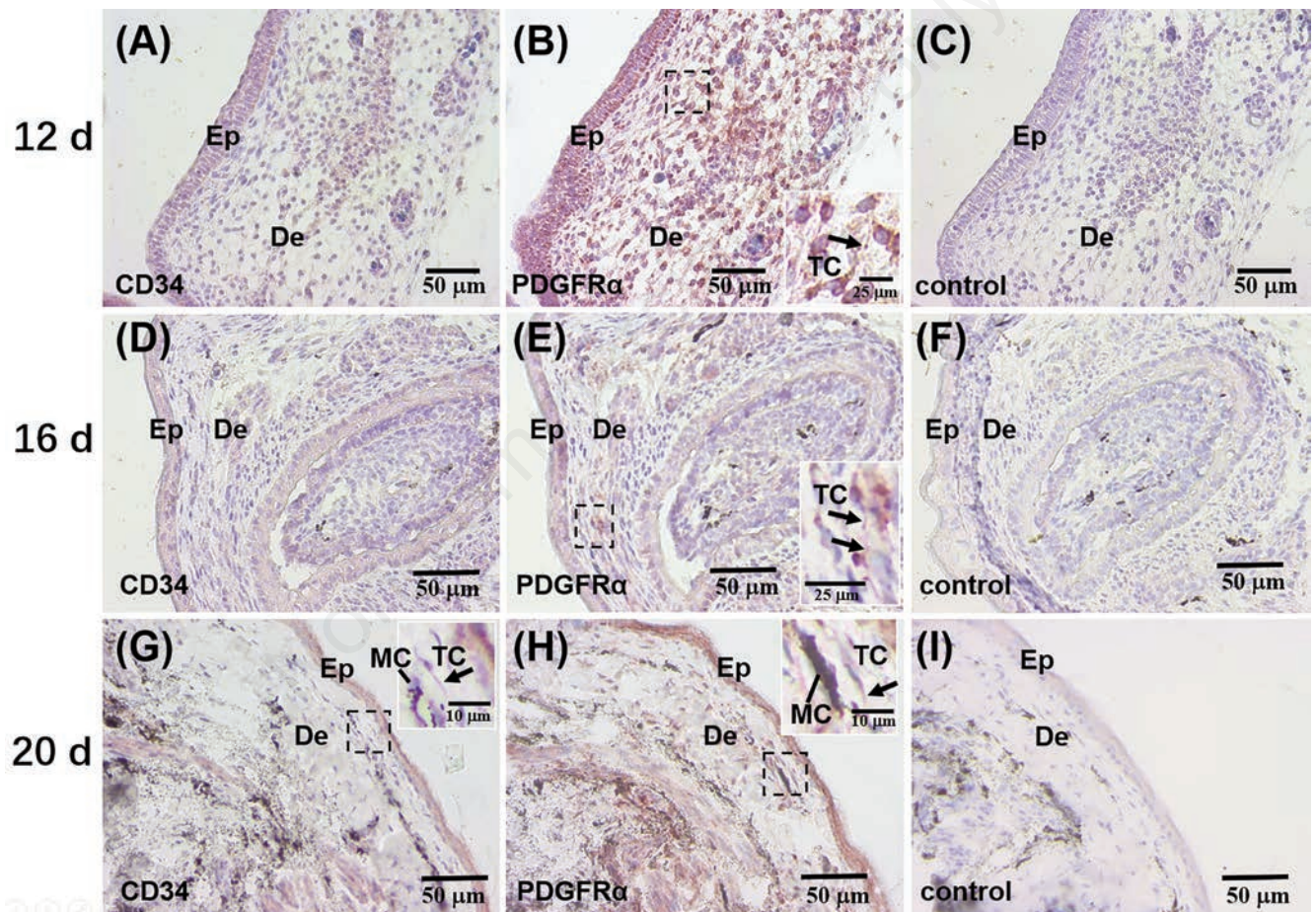


**Figure 2.** Light microscopy microphotographs showing telocytes (TCs) by immunohistochemistry in the skin of late embryo of the silky fowl. **A-I)** are serial sections from the identical skin sample of an incubation 12, 16 and 20-day embryo, respectively. **A)** TCs showing faintly immunopositive by CD34 immunohistochemistry. **B)** TCs showing positive by PDGFR $\alpha$  immunohistochemistry; the inset from the black dashed line boxed area exhibits a PDGFR $\alpha$ <sup>+</sup> TCs with a slender and toruliform telopode (black arrow). **C)** Negative control without primary antibody. **D)** TCs showing faintly positive by CD34 immunohistochemistry. **E)** TCs showing positive by PDGFR $\alpha$  immunohistochemistry. The inset from the black dashed line boxed area exhibits a PDGFR $\alpha$ <sup>+</sup> TC with slender and toruliform telopodes (black arrows). **F)** Negative control without primary antibody. **G)** TCs showing positive by CD34 immunohistochemistry. The inset from the black dashed line boxed area exhibits a CD34<sup>+</sup> TC with slender telopodes (black arrow); a melanocyte (MC) is observed near the TCs. **H)** TCs showing positive by PDGFR $\alpha$  immunohistochemistry. The inset from the black dashed line boxed area exhibits a PDGFR $\alpha$ <sup>+</sup> TC with slender telopodes (black arrows); a melanocyte (MC) is also observed in close proximity to the TC. **I)** Negative control without primary antibody. Ep, epidermis; De, dermis.



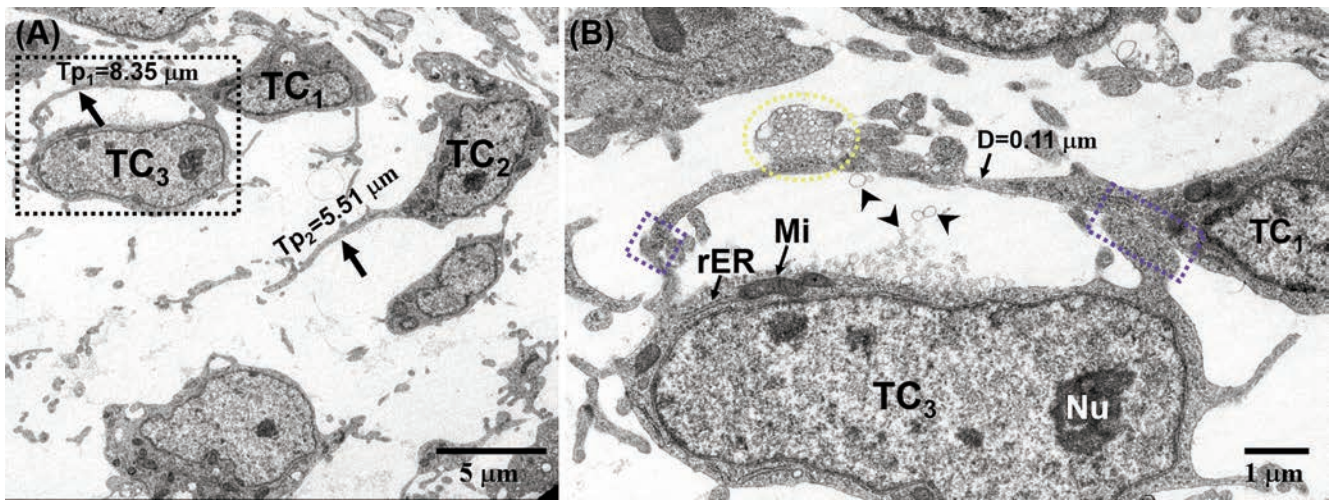


**Figure 3.** TEM micrographs of the skin of incubation 12-day embryo of the silky fowl. **A)** Three telocytes (TCs) with thin and long telopodes (Tps, black arrows) ( $Tp_1=8.35 \mu\text{m}$ ;  $Tp_2=5.51 \mu\text{m}$ ) are observed in the dermis. **B)** High-magnification TEM micrograph of the black dashed line boxed area shown in (A) with details of telopodes and the surrounding niche; the telopodes is thin (diameter =  $0.11 \mu\text{m}$ ); the nucleus of TCs is big and occupy most of the cell body; the nucleus contains a clear and electron-dense nucleolus (Nu); the cytoplasm is scarce within organelles, mitochondria (Mi) and rough endoplasmic reticulum (rER); the homocellular close contacts (the blue dashed line boxed areas) were observed between telopodes; the multivesicular body (the yellow dashed line boxed areas) is observed in close proximity to the Tps; several free exosomes (arrowheads) are also observed near the telopod.

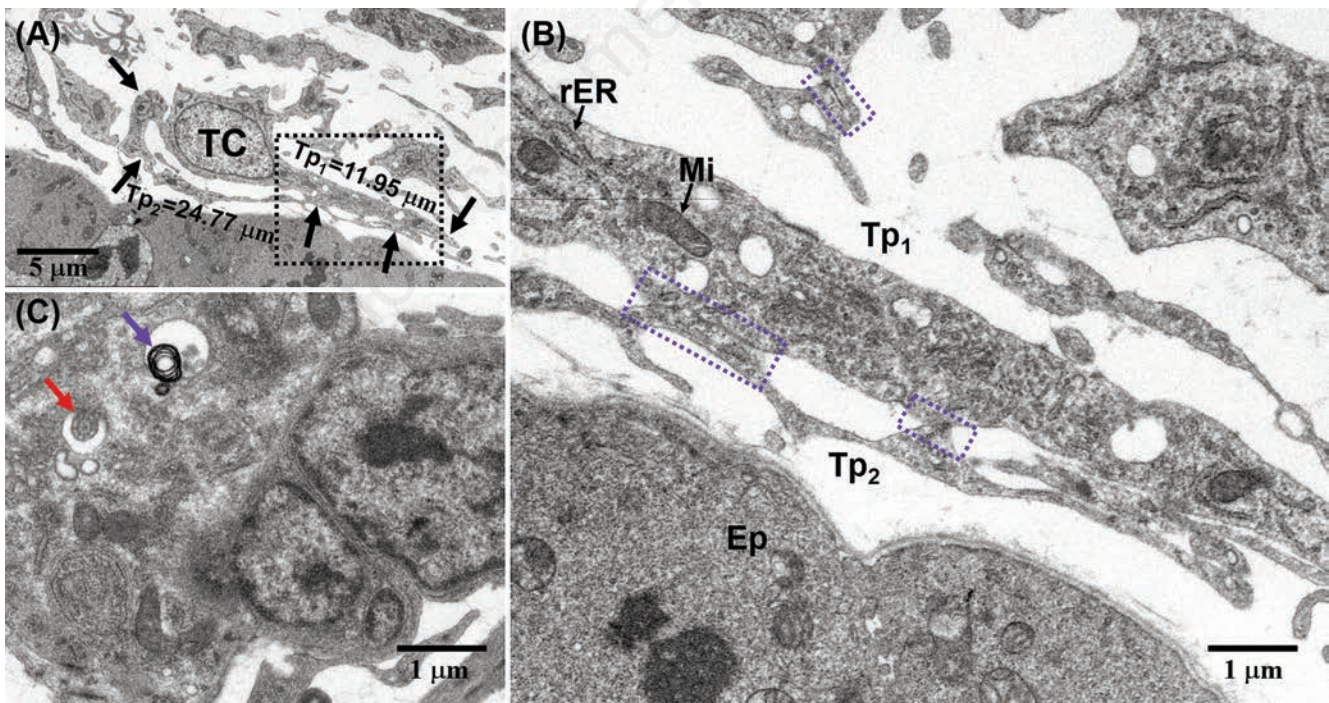


**Figure 4.** TEM micrographs of the skin of incubation 12-day embryo in the silky fowl. **A)** A telocyte (TC) with two thin and long telopodes (Tps) (black arrows, lengths are  $11.95 \mu\text{m}$  and  $24.77 \mu\text{m}$ , respectively.) **B)** High-magnification TEM micrograph of the black dashed line boxed area shown in (A) with details of Tps; the organelles, mitochondria (Mi) and rough endoplasmic reticulum (rER) were observed in the Tps; the homocellular close contacts (the blue dashed line boxed areas) were observed between Tps; Ep, epidermis. **C)** The lamellar bodies (blue arrow) and cilium (red arrow) were observed.



In the embryonic skin at the 16<sup>th</sup> day of incubation, TCs were observed in the dermis (Figures 5 and 6). TCs also had spindle bodies with very thin and long Tps. The mean length of the Tps was 11.18  $\mu\text{m}$  ( $n=5$ ). The thickness of thin podomers and thick podoms of Tps was 0.02-0.03  $\mu\text{m}$  and 3.43  $\mu\text{m}$ , respectively (Figure 5 A,B). The thick podom of Tps contained dense mitochondria and rough endoplasmic reticulum (Figures 5A and 6A). Some of the Tps were branched (Figure 6A). The extracellular multivesicular bodies with 1.27 $\pm$ 0.24  $\mu\text{m}$  ( $n=4$ ) in diameters were observed closely attached to the Tps (Figures 5A,C and 6A). The intracellular multivesicular bodies with 0.67 $\pm$ 0.26  $\mu\text{m}$  ( $n=2$ ) in diameters were also observed in the cytoplasm of TCs (Figure 5C). The exosomes with 0.17 $\pm$ 0.07  $\mu\text{m}$  ( $n=6$ ) in diameters were observed in close proximity to the Tps. In addition, the discrete caveolae were observed in the Tps (Figure 6A). TCs/Tps frequently established homocellular close contacts (Figures 5A and 6A). Plasmalemmal adhesion was also observed between Tps (Figure 6A). Melanocytes with oval and electron-dense melanosomes were observed close to the Tps (Figure 6B).

In the embryonic skin at the 20<sup>th</sup> day of incubation, TCs were observed in the dermis (Figures 7 and 8). TCs had oval cell bodies, and thin and long Tps. The mean length of the Tps was 17.49  $\mu\text{m}$  ( $n=8$ ). The thickness of the Tps in the thin podomer segments was 0.02  $\mu\text{m}$ . In the thick podom segments, the thickness of Tps was 0.58  $\mu\text{m}$ . The homocellular close contacts were observed between

Tps, and Tps and cell bodies (Figure 7A). An extracellular multivesicular body with 0.92  $\mu\text{m}$  ( $n=1$ ) in diameter was observed in close proximity to the Tps (Figure 7B). The exosomes with 0.10 $\pm$ 0.02  $\mu\text{m}$  ( $n=4$ ) in diameters were also observed in close proximity to the Tps. In addition, Tps were frequently found in close proximity to the melanocytes (Figures 7A and 8). Importantly, Tps and melanocytes formed heterocellular close contacts (Figure 8 B,C). In addition, an extracellular multivesicular body with 0.64  $\mu\text{m}$  ( $n=1$ ) in diameter was observed between Tps and melanocytes (Figure 8B). The extracellular multivesicular body was close to both the Tps and the melanocytes.

### Location relationships between TCs/Tps and melanocytes of skin at different developmental periods of late silky fowl embryos

After H&E staining and IHC, the melanocytes were not observed in the embryonic skin at the 12<sup>th</sup> day of incubation. Melanocytes/melanin were observed at the 16<sup>th</sup> day of incubation, but were still sparse. It was not until the 20<sup>th</sup> day of incubation that the melanocytes/melanin were denser (Figures 1 and 2). With the embryo developing, there was a pattern of distribution of melanocytes from absent to present and from sparse to dense in the skin (Figures 1 and 2). In addition, melanocytes were observed in close proximity to the Tps (Figures 2 G,H).

By TEM, the melanocytes were not observed in the embryonic

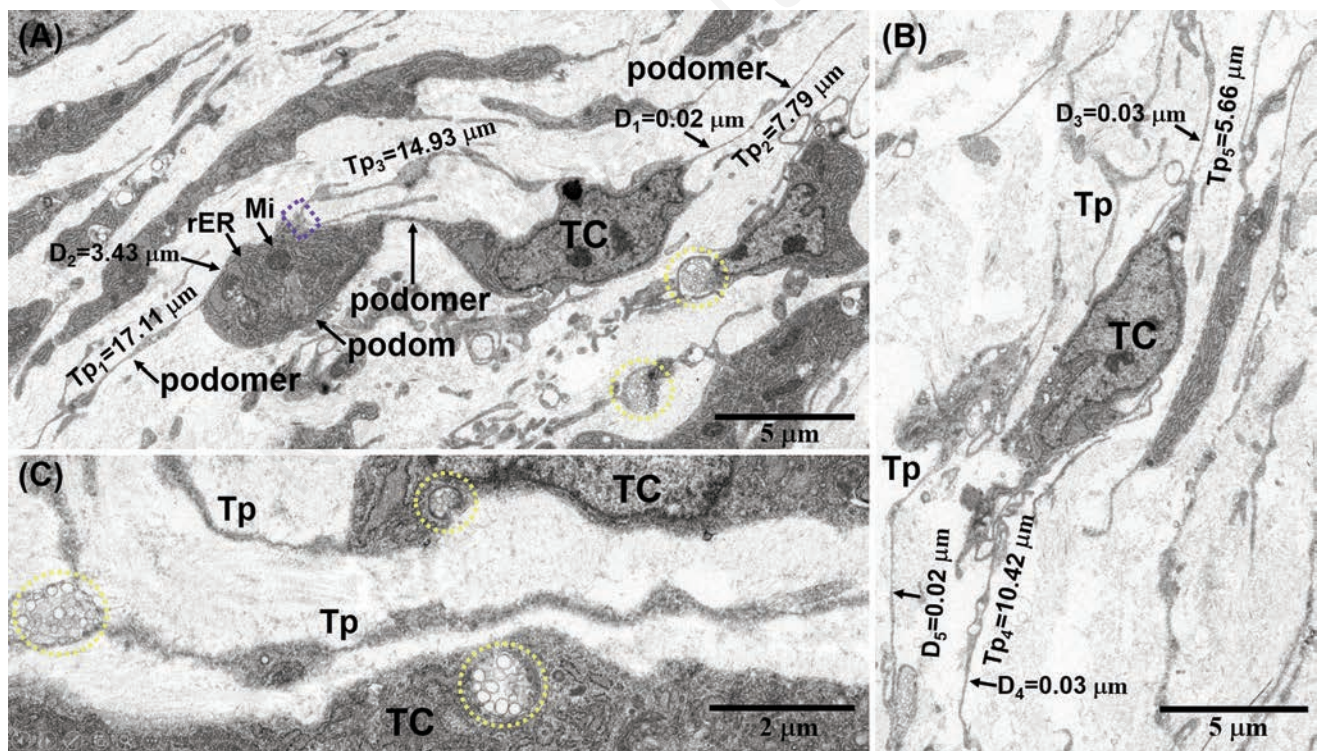


**Figure 5.** TEM micrographs of the skin of incubation 16-day embryo in the silky fowl. **A)** Telocytes (TCs) with long telopodes (Tps) are observed in the dermis of 16-day embryo in the silky fowl; a TC possesses two long Tps (The lengths of Tp<sub>1</sub> and Tp<sub>2</sub> are 17.11  $\mu\text{m}$  and 7.79  $\mu\text{m}$ ); the Tps appear as moniform aspect with various thickness; Tps consist of thick podom (diameter = 3.43  $\mu\text{m}$ ) and thin podomer (diameter = 0.02  $\mu\text{m}$ ); the thick podom contains the organelles, mitochondria (Mi) and rough endoplasmic reticulum (rER); the homocellular close contact (the blue dashed line boxed area) is observed between Tps; the extracellular multivesicular bodies (the yellow dashed line boxed areas) were observed in close proximity to Tps. **B)** Telocytes (TCs) are observed in the dermis; the TCs possess very thin and long the telopodes (Tps); the diameters of Tps are 0.02 and 0.03  $\mu\text{m}$ , respectively; the lengths of Tps are 5.66  $\mu\text{m}$  and 10.42  $\mu\text{m}$ , respectively. **C)** The extracellular and intracellular multivesicular bodies (the yellow dashed line boxed areas) were frequently observed in close proximity to Tps and in the cytoplasm of TCs, respectively.



skin at the 12<sup>th</sup> day of incubation (Figures 3 and 4). Rarely, the melanocytes containing electron-dense melanosomes were observed in the embryonic skin at the 16<sup>th</sup> day of incubation (Figure 6B). Furthermore, the melanocytes were located close to the Tps. In the embryonic skin at the 20<sup>th</sup> day of incubation, the melanocytes were found to contain many oval and electron-dense melanosomes (Figures 7 and 8). In particular, the melanocytes established close contacts with the neighbouring TCs/Tps (Figure 8). In addition, extracellular multivesicular bodies were observed between melanocytes and TCs/Tps, which remained close to each other (Figure 8 B,C).

## Discussion

TCs have been found in virous organs of human and animals in previous studies. Data on TCs in birds is very limited. Currently, several studies on TCs in the adult birds, including chickens, ducks and geese, have been performed.<sup>24-28</sup> These results demonstrated that avian TCs have unique structural features compared to the canonical TCs in other animals. In general, avian TCs have 2-3 very long and thin cellular prolongations - Tps, which appear as moniliform aspect with varying thickness. In other words, Tps contain the thick segments - podoms and the thin segments - podomers. The podoms and podomers are alternately distributed. In addition, avian TCs and their Tps established homocellular con-

tacts, and also establish heterocellular contacts with neighbouring different cell types/non-cell structures.

In general, in normal skin, TCs were located in the dermis and had specific spatial relationships with different dermal structures such as blood vessels, hair follicles, *arrector pili* muscles, cutaneous glands.<sup>29,30</sup> In the dermis of adult silky fowl, the structural characteristics of TCs were consistent with the canonical TCs.<sup>24</sup> TCs and their Tps were frequently observed in close proximity to neighbouring cell types or non-cell structures, such as adipocytes, collagen fibres, and capillaries. Homocellular contacts by plasmalemmal adhesion between TCs/Tps were observed. Moreover, the heterocellular close contacts by point contacts were observed between TCs/Tps and surrounding cells, including stem cells and melanocytes. The multivesicular bodies, including exosomes, released from TCs/Tps were observed in close proximity to TCs/Tps. The study provided histological evidence for TCs the involvement of TCs in intercellular communication in avian skin.

In the present study, TCs were described in the developing skin of the silky fowl. The morphological features of the embryonic TCs in the study were somewhat comparable to the TCs in other animals. Overall, they shared very similar ultrastructural features. Moreover, TCs and their Tps established structural relationships with surrounding cell types. Homocellular contacts between TCs and heterocellular contacts between TCs and neighbouring melanocytes were observed in the dermis. Through Tps and their homocellular and heterocellular contacts, TCs were organized in a

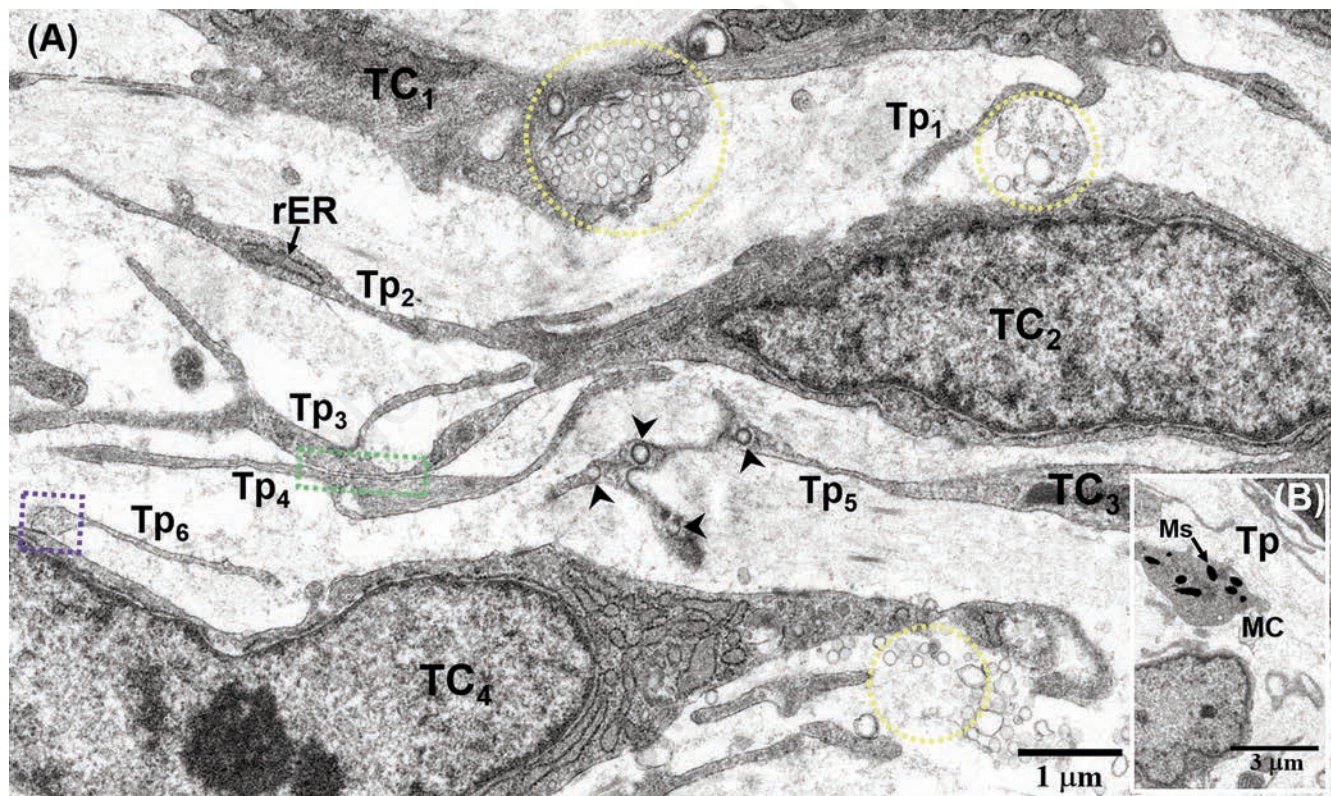


**Figure 6.** TEM micrographs of the skin of incubation 16-day embryo in the silky fowl. **A**) Telocytes (TCs) with thin and long telopodes (Tps) are observed in the dermis; TC<sub>2</sub> possesses a branching Tp<sub>3</sub>; the podom of Tp<sub>2</sub> contains the rough endoplasmic reticulum (rER); Tp<sub>5</sub> contains some small and rounded caveolae (black arrowheads); the multivesicular bodies (the yellow dashed line boxed areas) were frequently observed in close proximity to Tps; Tp<sub>6</sub> establishes homocellular close contact (the blue dashed line boxed area) with TC<sub>4</sub>; Tp<sub>3</sub> and Tp<sub>4</sub> establish homocellular structural relationship by plasmalemmal adhesion (the green dashed line boxed area). **B**) A melanocyte (MC) within oval and electron-dense melanosome (Ms) is observed near some Tps.



3D network and played a role in the mechanical support. The signal communication occurred between the TCs by the direct homocellular contacts.<sup>31</sup> Additionally, the extracellular vesicles and free shedding exosomes were also observed in close proximity to TCs/Tps. These shed vesicles have been suggested to contain signalling molecules.<sup>32</sup> Thus, TCs had a paracrine function through the extracellular vesicles and free shedding exosomes. The paracrine function of TCs has been implicated in angiogenesis and/or vascular homeostasis, and dermal tissue remodelling/repair processes.<sup>29</sup> These data may also be useful for understanding the role of TCs in pathologies such as scleroderma, multiple sclerosis, psoriasis, *etc.*<sup>33</sup> Therefore, TCs exerted their cellular effect in intercellular signalling and communication either through instituting cellular contact (physically) or through paracrine mode (chemically).<sup>31,32</sup> Recently, TCs studies involving avian embryos are available. In the Japanese quail embryo, TCs were observed in the mucosa, submucosa and muscle layers of the caecal proximal part at 13<sup>th</sup> embryonic day by IHC and TEM.<sup>34</sup> In the oesophagus of quail embryos, at the 5<sup>th</sup> to 8<sup>th</sup>, 15<sup>th</sup> days of incubation, TCs were identified in the walls of the esophagus by histochemistry, IHC and TEM.<sup>35</sup> TCs were recognized in the laminae propria, submucosa and muscular layer of oesophagus. TCs exhibited high affinity for PAS and were immunopositive for CD34 and VEGF by IHC. TCs were VEGF<sup>+</sup>, suggesting that TCs may promote endothelial cell proliferation and angiogenesis.<sup>36</sup>

In adult silky fowl, our current study demonstrated that TCs

are located in the dermis and were immunopositive for CD34, c-Kit, and PDGFR $\alpha$ .<sup>24</sup> TCs still do not have a specific marker. Endothelial progenitors show CD34<sup>+</sup> and PDGFR $\alpha$ . Fibroblasts show CD34<sup>-</sup> and PDGFR $\alpha$ <sup>+</sup>. TCs show CD34<sup>+</sup> and PDGFR $\alpha$ <sup>+</sup>.<sup>37</sup> Therefore, many previously published papers consider CD34 and PDGFR $\alpha$  to be a relatively reliable marker of TCs. In the present study, TCs showed CD34 immunoreactivity in the embryonic skin at the 20<sup>th</sup> day of incubation. CD34 is a member of a family of transmembrane sialomucin proteins, and it is a common marker for haematopoietic stem cells, haematopoietic progenitor cells, as well as non-haematopoietic cells such as epithelial and endothelial progenitors, multipotent mesenchymal stromal cells. Both endothelial progenitors and TCs express CD34 and they share similar morphology. But endothelial cells are components of blood vessels and lymphatic vessels. Therefore, it is possible to distinguish between endothelial cells and TCs by the presence or absence of haemocytes in elongated CD34<sup>+</sup> cells. CD34 is critical for adhesion molecules, proliferation and blocking differentiation of stem and progenitor cells.<sup>35</sup> TCs of embryonic skin exhibited CD34 immunoreactivity. It is suggested that TCs play an essential role in angiogenesis and morphogenesis.<sup>35</sup>

In addition, in the present study, TCs exhibited PDGFR $\alpha$  immunoreactivity. PDGF and its receptors PDGFR have served as prototypes for growth factor and receptor tyrosine kinase function. Studies of PDGF and PDGFR in animal development have revealed roles for PDGFR $\alpha$  signalling in gastrulation and in the

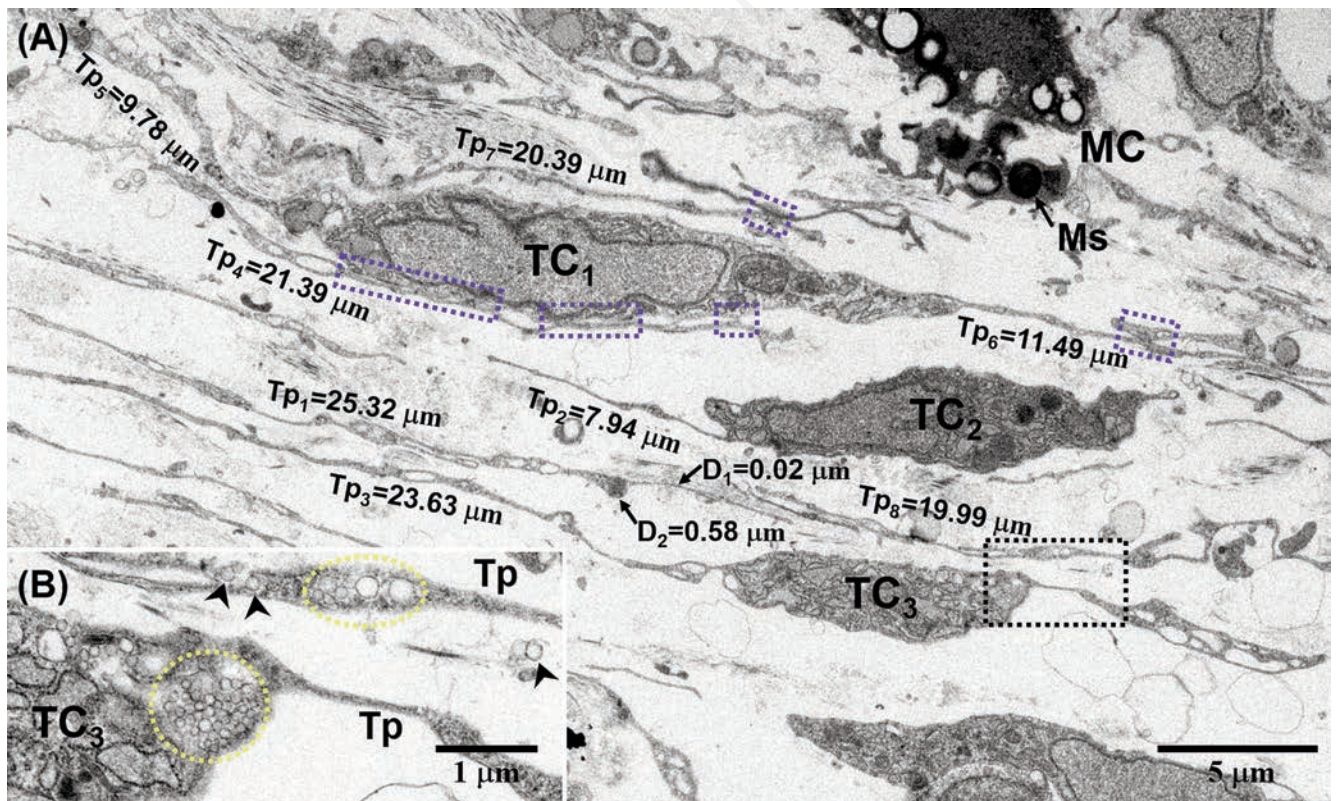


**Figure 7.** TEM micrographs of the skin of incubation 20-day embryo in the silky fowl. **A**) Telocytes (TCs) with thin and long telopodes (Tps) are observed in the dermis; the lengths of Tps of TCs are measured by ImageJ software; also, the Tps of TCs exhibit moniliform aspect with different diameters, thin podomer ( $D_1 = 0.02 \mu\text{m}$ ) and thick podomer ( $D_2 = 0.58 \mu\text{m}$ ); TCs establish frequently homocellular close contact (the blue dashed line boxed area); a melanocyte (MC) within rounded and electron-dense melanosome (Ms) is observed near the Tps. **B**) Tps contain intracellular multivesicular bodies (the yellow dashed line boxed area); the free shedding exosomes (black arrow heads) are observed in close proximity to the Tps.



development of the cranial and cardiac neural crest, gonads, lung, intestine, skin, CNS, and skeleton.<sup>38</sup> In the skin, PDGFR $\alpha$ <sup>+</sup> mesenchymal cells are recruited to hair follicles to become dermal papillae and dermal sheath.<sup>39</sup> The dermal sheath is a smooth muscle that drives follicles regression for reuniting niche and stem cells in order to regenerate tissue structure during homeostasis.<sup>40</sup> It is suggested that these PDGFR $\alpha$ <sup>+</sup> mesenchymal cells in skin are exactly the new type of mesenchymal cells – TCs. Moreover, our results had confirmed that TCs are located in the dermis of silky fowl at developmental embryos. Thus, PDGFR $\alpha$ <sup>+</sup> TCs play a critical role in the development of the dermis and hair follicles. TCs serve as cellular players to participate in renewal or repair processes after skin injury.<sup>41</sup> TCs may be indispensable for skin wound repair and hair follicle regeneration. It is tempting to speculate that TCs may be a novel potential target for therapeutic strategies aimed at enhancing skin repair, hair follicle regeneration and hair cycle regression after wounding in clinical application.<sup>42</sup> A study has demonstrated that TCs reduce the delay in wound healing and the inflammatory responses induced by LPS may be mediated by inflammatory inhibition, thereby restricting apoptosis and promot-

ing migration of the major component cell types in the skin of mice.<sup>43</sup> In perspective, these findings may have important implications in the field of skin regenerative medicine.<sup>44</sup> The location and structural relationships between TCs and melanocytes supported the note that the TCs appear to be involved in the melanogenesis as we observed close contacts between the Tps and melanocytes. Cutaneous TCs have been demonstrated to have an endocytic function, intake pigment of hemosiderin and melanin,<sup>45</sup> or transfer pigment to other cells.<sup>24</sup> The locations of melanin may be regulated by TCs. Our findings confirmed that the locations, immunophenotypes, and structural characteristics of TCs in the skin of embryos of the silky fowl at the later stages of incubation. Furthermore, the structural relationships between TCs and surrounding cell types/structures, including melanocytes, were observed in the skin of late embryo of the silky fowl. TCs with canonical morphological features and immunophenotypes were present in developing skin. The study revealed differences in either CD34/PDGFR $\alpha$  immunopositivity or structural characteristics of TCs with skin development. The putative role of TCs is the regulation of skin morphogenesis through both direct intercellular contacts and trans-

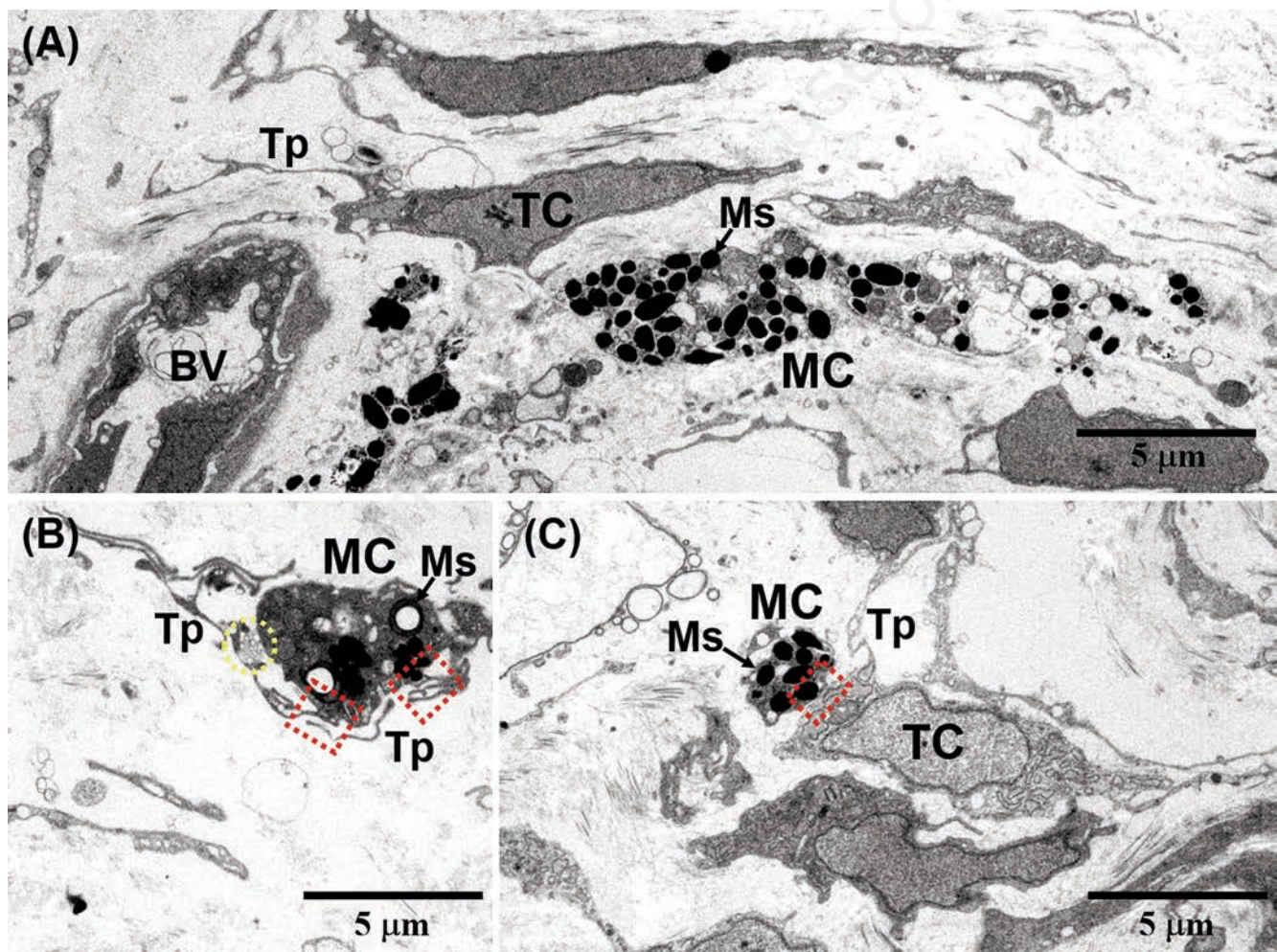


**Figure 8.** TEM micrographs of the skin of incubation 20-day embryo in the silky fowl. **A)** Telocytes (TCs) with thin and long telopodes (Tps) are observed in the vicinity of blood vessel (BV); TCs are also observed near neighboring melanocytes (MC) that containing many rounded and electron-dense melanosomes (Ms). **B)** Tps establish heterocellular close contacts (the red dashed line boxed area) with melanocyte (MC); the extracellular multivesicular bodies (the yellow dashed line boxed area) are observed between Tps and MC. **C)** The heterocellular close contacts (the red dashed line boxed area) are also observed between another TC and MC.



fer of extracellular vesicles to neighbouring cells.<sup>46</sup> TCs were suggested to be involved in skin and its accessory organs morphogenesis and regeneration/repair processes. These results underline the importance of expanding our knowledge of the biological properties of TCs and their role as key regulators of the 3D architecture of the organs. Furthermore, it would be attractive to consider that augmenting dermal TCs' presence/density could become an attractive therapeutic alternative for treating various skin wounds and defects in regenerative medicine.<sup>12,47</sup> TCs may have a potential in clinical application for treating skin wound and defects in regenerative medicine.

## References

- Popescu LM, Fausone-Pellegrini MS. TELOCYTES - a case of serendipity: the winding way from Interstitial Cells of Cajal (ICC), via Interstitial Cajal-Like Cells (ICLC) to TELOCYTES. *J Cell Mol Med* 2010;14:729-40.
- Crețoiu D, Crețoiu SM, Simionescu AA, Popescu LM. Telocytes, a distinct type of cell among the stromal cells present in the lamina propria of jejunum. *Histol Histopathol* 2012;27:1067-78.
- Kondo A, Kaestner KH. Emerging diverse roles of telocytes. *Development* 2019;146:dev175018.
- Crețoiu SM. Telocytes and other interstitial cells: from structure to function. *Int J Mol Sci* 2021;22:5271.
- Vannucchi MG. Telocytes and macrophages in the gut: from morphology to function, do the two cell types interact with each other? which helps which? *Int J Mol Sci* 2022;23:8435.
- Díaz-Flores L, Gutiérrez R, Díaz-Flores L Jr, Gómez MG, Sáez FJ, Madrid JF. Behaviour of telocytes during physiopathological activation. *Semin Cell Dev Biol* 2016;55:50-61.
- Zhao J, Birjandi AA, Ahmed M, Redhead Y, Olea JV, Sharpe P. Telocytes regulate macrophages in periodontal disease. *eLife* 2022;11:e72128.
- Rosa I, Marini M, Manetti M. Telocytes: An emerging component of stem cell niche microenvironment. *J Histochem Cytochem* 2021;69:795-818.
- Bahar Halpern K, Massalha H, Zwick RK, Moor AE, Castillo-Azofeifa D, Rozenberg M, et al. Lgr5+telocytes are a signaling source at the intestinal villus tip. *Nat Commun* 2020;11:1936.
- Bernier-Latmani J, Mauri C, Marcone R, Renevey F, Durot S, He L, et al. ADAMTS18+ villus tip telocytes maintain a polarized VEGFA signaling domain and fenestrations in nutrient-absorbing intestinal blood vessels. *Nat Commun* 2022;13:3983.
- Shoshkes-Carmel M, Wang YJ, Wangenstein KJ, Tóth B, Kondo A, Massasa EE, et al. Subepithelial telocytes are an important source of Wnts that supports intestinal crypts. *Nature* 2018;557:242-6.
- Manole CG, Gherghiceanu M, Ceafalan LC, Hinescu ME. Dermal telocytes: a different viewpoint of skin repairing and regeneration. *Cells* 2022;11:3903.
- Aleksandrovykh V, Gil K. Telocytes in the tumor microenvironment. *Adv Exp Med Biol* 2021;1329:205-16.
- Luan C, Xu Y. Matrix metalloproteinase gene mutations and bioinformatics of telocytes in hepatocellular carcinoma. *Cell Biol Int* 2023;47:110-22.
- Díaz-Flores L, Gutiérrez R, González-Gómez M, García MDP, Palmas M, Carrasco JL, et al. Delimiting CD34+ stromal cells/telocytes are resident mesenchymal cells that participate in neovessel formation in skin Kaposi sarcoma. *Int J Mol Sci* 2023;24:3793.
- Xu T, Zhang H, Zhu Z. Telocytes and endometriosis. *Arch Gynecol Obstet* 2023;307:39-49.
- Karasu Y, Önal D, Zırh S, Yersal N, Korkmaz H, Üstün Y, et al. Role of telocytes in the pathogenesis of ectopic pregnancy. *Eur Rev Med Pharmacol Sci* 2022;26:110-9.
- Wei XJ, Chen TQ, Yang XJ. Telocytes in fibrosis diseases: from current findings to future clinical perspectives. *Cell Transplant* 2022;31:9636897221105252.
- Díaz-Flores L, Gutiérrez R, García MP, González-Gómez M, Rodríguez-Rodríguez R, Hernández-León N, et al. Cd34+ stromal cells/telocytes in normal and pathological skin. *Int J Mol Sci* 2021;22:7342.
- Moisan F, Oucherif S, Kaulanjan-Checkmodine P, Prey S, Rousseau B, Bonneau M, et al. Critical role of Aquaporin-1 and telocytes in infantile hemangioma response to propranolol beta blockade. *Proc Natl Acad Sci USA* 2021;118:e2018690118.
- Langlois MJ, Servant R, Reyes Nicolás V, Jones C, Roy SAB, Paquet M, et al. Loss of PTEN signaling in foxl1+ mesenchymal telocytes initiates spontaneous colonic neoplasia in mice. *Cell Mol Gastroenterol Hepatol* 2019;8: 530-3.
- Pomerleau V, Nicolas VR, Jurkovic CM, Fauchoux N, Lauzon MA, Boisvert FM, et al. FOXL1+ Telocytes in mouse colon orchestrate extracellular matrix biodynamics and wound repair resolution. *J Proteomics* 2023;271:104755.
- Crețoiu D, Radu BM, Banciu A, Banciu DD, Crețoiu SM. Telocytes heterogeneity: From cellular morphology to functional evidence. *Semin Cell Dev Biol* 2017;64:26-39.
- Chen X, Zeng J, Huang Y, Gong M, Ye Y, Zhao H, et al. Telocytes and their structural relationships with surrounding cell types in the skin of silky fowl by immunohistochemical, transmission electron microscopical and morphometric analysis. *Poult Sci* 2021;100:101367.
- Wang Q, Haseeb A, Meng X, Feng Y, Hussain A, Yang P. Telocytes in the esophageal wall of chickens: a tale of subepithelial telocytes. *Poult Sci* 2022;101:101859.
- Zhu X, Wang Q, Pawlicki P, Wang Z, Pawlicka B, Meng X, et al. Telocytes and their structural relationships with the sperm storage tube and surrounding cell types in the utero-vaginal junction of the chicken. *Front Vet Sci* 2022;9:852407.
- Mokhtar DM, Hussien MM. Cellular elements organization in the trachea of mallard (*Anas platyrhynchos*) with a special reference to its local immunological role. *Protoplasma* 2020;257:407-20.
- Anwar SM, Abd-Elhafeez HH, Abdel-Maksoud FM, Abdalla KEH. Morph-anatomic and histochemical study of ileum of goose (*Alopochen aegyptiacus*) with special references to immune cells, mucous and serous goblet cells, telocytes, and dark and light smooth muscle fibers. *Microsc Res Tech* 2021;84:1328-47.
- Kang Y, Zhu Z, Zheng Y, Wan W, Manole CG, Zhang Q. Skin telocytes versus fibroblasts: two distinct dermal cell populations. *J Cell Mol Med* 2015;19:2530-9.
- Meng X, Zhu Z, Ahmed N, Ma Q, Wang Q, Deng B, et al. Dermal microvascular units in domestic pigs (*Sus scrofa domestica*): role as transdermal passive immune channels. *Front Vet Sci* 2022;9:891286.
- Sayed RKA, Abd-El Aziz NA, Ibrahim IA, Mokhtar DM. Structural, ultrastructural, and functional aspects of the skin of the upper lip of silver carp (*Hypophthalmichthys molitrix*). *Microsc Res Tech* 2021;84:1821-33.
- Manole CG, Simionescu O. The cutaneous telocytes. *Adv Exp Med Biol* 2016;913:303-23.
- Crețoiu D, Gherghiceanu M, Hummel E, Zimmermann H, Simionescu O, Popescu LM. FIB-SEM tomography of human skin telocytes and their extracellular vesicles. *J Cell Mol Med* 2015;19:714-22.



34. AbuAli AM, Mokhtar DM, Ali RA, Wassif ET, Abdalla KEH. Cellular elements in the developing caecum of Japanese quail (*Coturnix coturnix japonica*): morphological, morphometrical, immunohistochemical and electron-microscopic studies. *Sci Rep* 2019;9:16241.
35. Soliman SA, Madkour FA. Developmental events and cellular changes occurred during esophageal development of quail embryos. *Sci Rep* 2021;11:7257.
36. Bojin FM, Gavriiuc OI, Cristea MI, Tanasie G, Tatu CS, Panaitescu C, et al. Telocytes within human skeletal muscle stem cell niche. *J Cell Mol Med* 2011;15:2269-72.
37. Romano E, Rosa I, Fioretto BS, Lucattelli E, Innocenti M, Ibba-Manneschi L, et al. A two-step immunomagnetic microbead-based method for the isolation of human primary skin telocytes/CD34+ stromal cells. *Int J Mol Sci* 2020;21:5877.
38. Andrae J, Gallini R, Betsholtz C. Role of platelet-derived growth factors in physiology and medicine. *Genes Dev* 2008;22:1276-312.
39. Karlsson L, Bondjers C, Betsholtz C. Roles for PDGF-A and sonic hedgehog in development of mesenchymal components of the hair follicle. *Development* 1999;126:2611-21.
40. Heitman N, Sennett R, Mok KW, Saxena N, Srivastava D, Martino P, et al. Dermal sheath contraction powers stem cell niche relocation during hair cycle regression. *Science* 2020;367:161-6.
41. Bei Y, Wang F, Yang C, Xiao J. Telocytes in regenerative medicine. *J Cell Mol Med* 2015;19:1441-54.
42. Bani D, Formigli L, Gherghiceanu M, Fausone-Pellegrini MS. Telocytes as supporting cells for myocardial tissue organization in developing and adult heart. *J Cell Mol Med* 2010;14:2531-8.
43. Wang L, Song D, Wei C, Chen C, Yang Y, Deng X, et al. Telocytes inhibited inflammatory factor expression and enhanced cell migration in LPS-induced skin wound healing models in vitro and in vivo. *J Transl Med* 2020;18:60.
44. Rosa I, Romano E, Fioretto BS, Guasti D, Ibba-Manneschi L, Matucci-Cerinic M, et al. Scleroderma-like impairment in the network of telocytes/CD34+ stromal cells in the experimental mouse model of bleomycin-induced dermal fibrosis. *Int J Mol Sci* 2021;22:12407.
45. Díaz-Flores L, Gutiérrez R, García MP, Sáez FJ, Aparicio F, Díaz-Flores L Jr, et al. Uptake and intracytoplasmic storage of pigmented particles by human CD34+ stromal cells/telocytes: endocytic property of telocytes. *J Cell Mol Med* 2014;18:2478-87.
46. Marini M, Manetti M, Rosa I, Ibba-Manneschi L, Sgambati E. Telocytes in human fetal skeletal muscle interstitium during early myogenesis. *Acta Histochem* 2018;120:397-404.
47. Bani D, Nistri S. New insights into the morphogenic role of stromal cells and their relevance for regenerative medicine. lessons from the heart. *J Cell Mol Med* 2014;18:363-70.

---

Received: 12 June 2024. Accepted: 23 September 2024.

This work is licensed under a Creative Commons Attribution-NonCommercial 4.0 International License (CC BY-NC 4.0).

©Copyright: the Author(s), 2024

Licensee PAGEPress, Italy

*European Journal of Histochemistry* 2024; 68:4089

doi:10.4081/ejh.2024.4089

*Publisher's note: all claims expressed in this article are solely those of the authors and do not necessarily represent those of their affiliated organizations, or those of the publisher, the editors and the reviewers. Any product that may be evaluated in this article or claim that may be made by its manufacturer is not guaranteed or endorsed by the publisher.*